

Accepted 2000 December 19 for publication in ApJ Letters

Substructure and dynamics of the Fornax Cluster

Michael J. Drinkwater

School of Physics, University of Melbourne, Victoria 3010, Australia

`mjdrin@unimelb.edu.au`

Michael D. Gregg

*Physics Dept., U.C. Davis, and IGPP, Lawrence Livermore National Laboratory, L-413,
Livermore, CA 94550, USA*

`gregg@igpp.ucllnl.org`

and

Matthew Colless

*Research School of Astronomy & Astrophysics, The Australian National University, Weston
Creek, ACT 2611, Australia*

`colless@mso.anu.edu.au`

ABSTRACT

We present the first dynamical analysis of a galaxy cluster to include a large fraction of dwarf galaxies. Our sample of 108 Fornax Cluster members measured with the UK Schmidt Telescope FLAIR-II spectrograph contains 55 dwarf galaxies ($15.5 > b_J > 18.0$ or $-16 > M_B > -13.5$). $H\alpha$ emission shows that $36 \pm 8\%$ of the dwarfs are star-forming, twice the fraction implied by morphological classifications. The total sample has a mean velocity of $1493 \pm 36 \text{ km s}^{-1}$ and a velocity dispersion of $374 \pm 26 \text{ km s}^{-1}$. The dwarf galaxies form a distinct population: their velocity dispersion ($429 \pm 41 \text{ km s}^{-1}$) is larger than that of the giants ($308 \pm 30 \text{ km s}^{-1}$) at the 98% confidence level. This suggests that the dwarf population is dominated by infalling objects whereas the giants are virialized.

The Fornax system has two components; the main Fornax Cluster centered on NGC 1399 with $\bar{cz} = 1478 \text{ km s}^{-1}$ and $\sigma_{cz} = 370 \text{ km s}^{-1}$, and a subcluster centered 3 degrees to the south-west including NGC 1316 with $\bar{cz} = 1583 \text{ km s}^{-1}$ and $\sigma_{cz} = 377 \text{ km s}^{-1}$. This partition is preferred over a single cluster at the 99% confidence level. The subcluster, a site of intense star formation, is bound to Fornax and probably infalling towards the cluster core for the first time. We discuss the implications of this

substructure for distance estimates of the Fornax Cluster. We determine the cluster mass profile using the method of Diaferio (1999), which does not assume a virialized sample. The mass within a projected radius of 1.4 Mpc is $(7 \pm 2) \times 10^{13} M_{\odot}$, and the mass-to-light ratio is $300 \pm 100 M_{\odot}/L_{\odot}$. The mass is consistent with values derived from the projected mass virial estimator and X-ray measurements at smaller radii.

Subject headings: galaxies: clusters: general — galaxies: clusters: individual (Fornax)
— cosmology: distance scale

1. Introduction

As the largest gravitationally bound systems in the Universe, clusters of galaxies offer unique constraints on the formation of large scale structure: models of galaxy infall onto clusters predict the velocity distributions of the infalling galaxies in terms of the density enhancement of the cluster and the cosmological mass density Ω_0 (Regos & Geller 1989). On smaller scales, clusters also provide important clues for theories of galaxy formation and evolution: the broader distribution of late-type (star-forming) galaxies compared to early-types in both poor clusters (e.g. Virgo, Huchra 1985) and rich clusters (e.g. Coma, Colless & Dunn 1996) is generally interpreted as evidence that the late-type galaxies are falling into the clusters for the first time, whereas the early types are an older, virialized population. These observations are based on luminous cluster galaxies ($M_B < -16$), even though they are greatly outnumbered by dwarf galaxies. Studies of the dwarf populations are limited to small samples in nearby clusters and groups, such as the Fornax Cluster (Held & Mould 1994) and the Sculptor and Centaurus A groups (Côté et al. 1997). In these studies, the dwarfs had more extended velocity and spatial distributions than the giants, but not at statistically significant levels. It is timely to investigate the behavior of dwarfs in clusters using larger samples, as numerical simulations of cluster formation can now resolve the formation of dark matter halos the size of dwarf galaxies (Ghigna et al. 2001).

We present a dynamical study of the Fornax Cluster, a nearby poor, but relatively dense cluster. Our sample includes a significant number of dwarf galaxies which form a distinct population kinematically. We find strong evidence that Fornax has a distinct subcluster containing a high concentration of star-forming galaxies. For our analysis we adopt a cluster distance of 20 Mpc (Mould et al. 2000, but see discussion below).

2. Galaxy Sample

Our analysis is based on a large study (Drinkwater et al. 2001) of the Fornax Cluster made with the FLAIR-II spectrograph on the UK Schmidt Telescope (UKST). We obtained redshifts for 516 galaxies with $b_J \leq 18$ in a $5.8 \times 5.8 \text{ deg}^2$ field centered on the Fornax Cluster. Most of the the targets (426 or $\approx 30\%$ of all galaxies in the field with $16.5 < b_J < 18.0$) were compact galaxies (scale

lengths ≤ 4 arcseconds) selected from a digitized UKST plate to search for new compact cluster members. The spectra have a resolution of 13\AA (velocity uncertainty $\Delta v = 50\text{ km s}^{-1}$). Eighteen were confirmed as cluster members, nine being new compact cluster dwarfs (Drinkwater & Gregg 1998). We also obtained 5.3\AA resolution spectra ($\Delta v = 30\text{ km s}^{-1}$) for a sample of 90 galaxies listed as probable cluster members in the Fornax Cluster Catalog (Ferguson 1989, FCC); this is 54% of the FCC members with $b_J < 18$. All 90 were confirmed as cluster members, giving a total sample of 108. The 53 galaxies with $b_J < 15.5$ ($M_B < -16$) we classify as giants and the remainder (55) as dwarfs. We also spectroscopically classify each galaxy as late-type or early-type; the 42 galaxies with $H\alpha$ emission equivalent width greater than 1\AA (a 3σ detection) were classified as late and the remainder (66) as early. Of the 43 dwarf galaxies with early-type morphological classifications in the FCC, 11 had enough $H\alpha$ emission to be reclassified by this criterion, so that $36 \pm 8\%$ of the dwarfs are spectroscopic late-types compared to 18% based on morphological classifications. The implications of this observation on the evolution of star formation in dwarf galaxies are discussed by Drinkwater et al. (2001).

3. Evidence for substructure

The Fornax Cluster has previously been noted for its relatively smooth Gaussian velocity distribution (Madore et al. 1999). Using the W test on our data for Fornax we find that the total sample of 108 galaxies has a velocity distribution that is marginally non-Gaussian (at the 91% confidence level), but the late/early and giant/dwarf subsamples are all consistent with Gaussians at the 2σ level (Fig. 1a,b). The total sample has a mean velocity of $1493 \pm 36\text{ km s}^{-1}$ and a velocity dispersion of $374 \pm 26\text{ km s}^{-1}$, in agreement with other work (see Drinkwater et al. 2000). Using the t- and F-tests, we find no significant differences in the mean velocities of the different subsamples or the velocity dispersions of the early ($356 \pm 31\text{ km s}^{-1}$) and late type samples ($405 \pm 45\text{ km s}^{-1}$). There is, however, a significant difference (at the 98% level) in the velocity dispersions of the dwarfs ($429 \pm 41\text{ km s}^{-1}$) and the giants ($308 \pm 30\text{ km s}^{-1}$). This was suspected by Held & Mould (1994), but their sample was too small for a significant result. We discuss the implications of this observation in Section 5 below.

We applied the “ κ -test” of Colless & Dunn (1996) to the total sample to test for velocity substructure. This test takes groups of the N nearest neighbors to each galaxy and compares the velocity distribution of the group to that of the whole cluster. The test revealed substructure for the $N = 4$ case at the 96% significance level, notably for a group to the southwest of the cluster center. Fig. 2 shows an adaptively-smoothed projection of the galaxy number density onto a plane of velocity against distance along a diagonal vector running through the cluster center from South West to North East, chosen to isolate the group in the SW corner of the cluster. We used the KMM mixture modeling algorithm to locate the substructure. This algorithm searches for the maximum-likelihood partition of a cluster into a specified number of subclusters (see Colless & Dunn 1996). We used a coordinate system based on offsets in projected separation on the sky measured in arc

minutes from the position of NGC 1399 ($\alpha = 03:38:29.0$ $\delta = -35:27:01$ J2000). The KMM analysis identified a very robust partition of the sample into a 92-member cluster (“Fornax-main”) centered at $(3', 18', 1478 \text{ km s}^{-1})$, with $\sigma_v = 370 \text{ km s}^{-1}$ and a 16-member subcluster (“Fornax-SW”) at $(-168', -72', 1583 \text{ km s}^{-1})$ with $\sigma_v = 377 \text{ km s}^{-1}$. Fornax-main is centered near NGC 1399 while Fornax-SW is dominated by NGC 1316 (Fornax A); see Fig. 3. The estimated correct allocation rate was 99% and the partition was preferred over a single distribution at the 99% confidence level. A further partition of Fornax-main identified a high-velocity clump (including the probably infalling NGC 1404 and associated objects, see below) projected on the cluster center, but this partition was not significantly better than a single distribution.

The radial distribution of the 92 galaxies in the Fornax-main cluster alone is shown in Fig. 1(c,d). Even on removing the spiral-rich Fornax-SW subcluster, the remaining 29 late-type galaxies are much more extended than the 63 early-types (at a KS significance level of 99%). In addition, the Fornax-main sample is no longer well-described by a King profile (Ferguson 1989), excluded at a KS significance level of 90%. Comparison of the dwarf and giant distributions in Fornax-main (Fig. 1(d)) shows that the dwarfs are more spatially extended at a KS significance level of 94%.

4. Cluster Mass Profile

The distributions of galaxy velocities against projected radius from cluster centers are predicted to exhibit caustic structures due to the overlapping of shells of infalling galaxies (Regos & Geller 1989) but this has previously been detected only in the Coma cluster (Geller et al. 1999). We plot this distribution for Fornax in Fig. 4. A caustic-like structure is strongly suggested when we consider just the early-type galaxies (circles). If real, this is the first detection of caustic structure in such a poor cluster, but the numbers of galaxies are too low to accurately determine the location of the caustics. For comparison we plot one caustic curve for a model (Praton & Schneider 1994) with $\Omega_0 = 0.3$, $\sigma_v = 374 \text{ km s}^{-1}$ and a turn-around radius of 2.4 Mpc, corresponding to a cluster mass of $9 \times 10^{13} M_\odot$ and a virial radius of 0.7 Mpc.

Although the caustics are not well-defined, we can use the method of Diaferio (1999) to measure the cluster mass as it provides a robust estimate without making assumptions of dynamical equilibrium. Briefly, the method works by defining caustic-like curves of the velocity amplitude $\mathcal{A}(r)$ as shown in Fig. 4. The amplitude is defined by the points where the galaxy density falls below a threshold κ , defined to minimize the difference between the escape velocities calculated from $\mathcal{A}(r)$ and estimated from the central velocity dispersion. The amplitude profile is then integrated to yield the mass profile $GM(< r) = \frac{1}{2} \int_0^r \mathcal{A}^2(x) dx$, also shown in Fig. 4. At small radii the resulting mass profile agrees well with independent estimates from X-ray measurements at the center of the cluster. The total enclosed mass at a radius of 1.4 Mpc is $(7 \pm 2) \times 10^{13} M_\odot$. Integrating the blue light from all galaxies out to the same radius we get $L_{1.4} = 2 \times 10^{11} L_\odot$ and a mass-to-light ratio of $300 \pm 100 M_\odot/L_\odot$, in the normal range for clusters (Bahcall et al. 2000). Limiting the analysis to the 92 galaxies of the main subcluster we obtain a slightly smaller mass of $(5 \pm 2) \times 10^{13} M_\odot$.

We also estimated the cluster mass by applying the virial theorem to the early-type galaxies alone (Fig. 4). We used the mean of the projected-mass estimators for radial and isotropic orbits (see Heisler et al. 1985). Interestingly, the projected mass estimator based on the early-type galaxies alone converges to a mass of $9 \times 10^{13} M_{\odot}$ consistent with that found using the Diaferio method applied to all galaxies in the cluster. We also applied the virial (projected mass) estimator to the SW subcluster, obtaining a mass of $6 \times 10^{13} M_{\odot}$, but this is an upper limit as this subcluster is presumably not virialized. Alternatively, if it had the same mass-to-light ratio as the main cluster, its mass would be $2 \times 10^{13} M_{\odot}$.

5. Discussion

As the difference in velocity dispersions between the dwarfs ($429 \pm 41 \text{ km s}^{-1}$) and the giants ($308 \pm 30 \text{ km s}^{-1}$) is consistent with the expected ratio of $\sqrt{2}:1$ for infalling and virialized populations (Colless & Dunn 1996), we conclude that the dwarf population is dominated by infalling objects whereas the giants are virialized. The more extended spatial distribution of the dwarfs supports this conclusion. This is the first detection of such separation of cluster components by mass, and it is not consistent with numerical simulations of cluster formation which do not show any mass segregation in the velocity dispersions (Ghigna et al. 2001). An alternative explanation is that dynamical relaxation (e.g. by dynamical friction of the massive galaxies) could have caused the mass segregation. The timescale for this is ~ 2 Gyr for the Fornax Cluster. Even assuming the dwarfs are only 5 times less massive than the giants (for a mass-to-light ratio ten times that of the giants), relaxation would give a dwarf velocity dispersion $\sqrt{5}$ times that of the giants. We cannot rule out partial relaxation giving the observed ratio, but this requires fine tuning of the mass segregation compared to the picture of infalling/virialized samples which naturally predicts the $\sqrt{2}:1$ ratio observed here and in the Virgo and Coma clusters.

The Fornax-SW subcluster has a recession velocity ($105 \pm 102 \text{ km s}^{-1}$) greater than the Fornax-main cluster. We attempted to constrain the physical motion of the subcluster using a two-body model as in Colless & Dunn (1996). The small relative motion of the two components gave a range of possible solutions, both incoming and outgoing. All the solutions were bound. Assuming all projection angles are equally probable, the most likely solutions have Fornax-SW infalling at velocities of $100\text{--}500 \text{ km s}^{-1}$ at radii of $3.5\text{--}1.1 \text{ Mpc}$. An infalling solution is supported by individual galaxy properties: Fornax-SW is a site of intense star formation, containing 15% of all galaxies in the total Fornax sample, but 31% of the star-forming galaxies. This subcluster contains two of the four cluster galaxies with exceptionally high star-formation rates, NGC 1341 and FCC 33 (Figs. 2 and 3) and a large amount of neutral hydrogen (Putman et al. 1998), unlikely to have survived a passage through the cluster core. Furthermore, observations of Fornax A in the subcluster (Ekers et al. 1983) indicate that it has a projected velocity of approximately 80 km s^{-1} northwards, consistent with infall. Similarly, the subgroup seen in projection on the cluster core (seen in Fig. 2 at 450 km s^{-1}) is probably real and infalling, although it was not robustly identified by the KMM

algorithm. This group contains NGC 1404, which has a distorted X-ray envelope indicative of infall (Jones et al. 1997), and the irregular galaxy NGC 1427A, which shows signs of being disrupted by its first passage through the cluster (Chanamé, Infante, & Reisenegger 2000). The morphologies of both these galaxies are indicative of material blown off behind them as they move towards the cluster center.

The substructure that we have identified in Fornax bears on the determination of its Cepheid distance. There are now three Cepheid distances to spirals in the Fornax region: NGC 1365 at 18.6 Mpc (Madore et al. 1999), NGC 1326A at 18.7 Mpc (Prosser et al. 1999), and NGC 1425 at 22.2 Mpc (Mould et al. 2000). Mould et al. suggest that the mean of these (≈ 20 Mpc) be adopted, but this may still not yield an accurate cluster distance. Though seen in projection only $70'$ (~ 0.4 Mpc) from the cluster core and with a similar velocity, NGC 1365 (see Fig. 2) may be situated near the turn-around radius (~ 2 Mpc out or $\sim 10\%$ in distance), given the tendency of late-type galaxies to avoid the cluster core. If NGC 1365 were in the cluster core, it might be expected to show morphological peculiarities like spirals in Virgo, Coma, and other clusters (see Bravo-Alfaro et al. 2000), but it is symmetric at wavelengths from optical to 20 cm (Lindblad 1999). With an identical Cepheid distance, and as a member of the infalling Fornax-SW subgroup (Fig. 3), NGC 1326A is also a doubtful indicator of the distance to the Fornax core. NGC 1425 is perhaps a better gauge of the cluster distance, but it is 5.6 (~ 2 Mpc) or ~ 10 core radii removed from the cluster center; it is not even clear whether NGC 1425 belongs to Fornax or the nearby Eridanus cluster (Mould et al.). While a simpler system than the Virgo cluster, Fornax nevertheless presents its own difficulties for an accurate distance measurement using Cepheids; a secure result awaits observations of additional spirals unambiguously residing in the cluster core.

We are very grateful to B. Holman, M. Brown and the staff of the UKST for observing assistance and N. Ryan for the caustic calculations. We thank M. Geller, B. Moore, P. Thomas and R. Webster for helpful discussions. Part of this work was done at the Institute of Geophysics and Planetary Physics, under the auspices of the U.S. Department of Energy by Lawrence Livermore National Laboratory (contract W-7405-Eng-48). This material is based upon work supported by the National Science Foundation (grant 9970884).

REFERENCES

- Bahcall, N. A., Cen, R., Davé, R., Ostriker, J. P., & Yu, Q. 2000, *ApJ*, 541, 1
- Bravo-Alfaro, H., Cayatte, V., van Gorkom, J. H., & Balkowski, C. 2000, *AJ*, 119, 580
- Chanamé, J., Infante, L., & Reisenegger, A. 2000, *ApJ*, 530, 96
- Colless, M. & Dunn, A. M. 1996, *ApJ*, 458, 435
- Côté, S., Freeman, K. C., Carignan, C., & Quinn, P. J. 1997, *AJ*, 114, 1313

- Diaferio, A. 1999, MNRAS, 309, 610
- Drinkwater, M. J. & Gregg, M. D. 1998, MNRAS, 296, L15
- Drinkwater, M. J., Gregg, M. D., Holman, B. A., & Brown, M. R. 2001, submitted to MNRAS
- Drinkwater, M. J., et al. 2000, A&A, 355, 900
- Ekers, R. D., Goss, W. M., Wellington, K. J., Bosma, A., Smith, R. M., & Schweizer, F. 1983, A&A, 127, 361
- Ferguson, H. C. 1989, AJ, 98, 367
- Geller, M. J., Diaferio, A., & Kurtz, M. J. 1999, ApJ, 517, L23
- Ghigna, S., Moore, B., Governato, E., Lake, G., Quinn, T., & Stadel, J. 2001, in press
- Heisler, J., Tremaine, S., & Bahcall, J. N. 1985, ApJ, 298, 8
- Held, E. V. & Mould, J. R. 1994, AJ, 107, 1307
- Huchra, J. P. 1985, in ESO Workshop on the Virgo Cluster, 181
- Ikebe, Y., et al. 1996, Nature, 379, 427
- Jones, C., Stern, C., Forman, W., Breen, J., David, L., Tucker, W., & Franx, M. 1997, ApJ, 482, 143
- Lindblad, P. O. 1999, A&A Rev., 9, 221
- Madore, B. F., et al. 1999, ApJ, 515, 29
- Mould, J. R., et al. 2000, ApJ, 528, 655
- Praton, E. A. & Schneider, S. E. 1994, ApJ, 422, 46
- Prosser, C. F., et al. 1999, ApJ, 525, 80
- Putman, M. E., Bureau, M., Mould, J. R., Staveley-Smith, L., & Freeman, K. C. 1998, AJ, 115, 2345
- Regos, E. & Geller, M. J. 1989, AJ, 98, 755

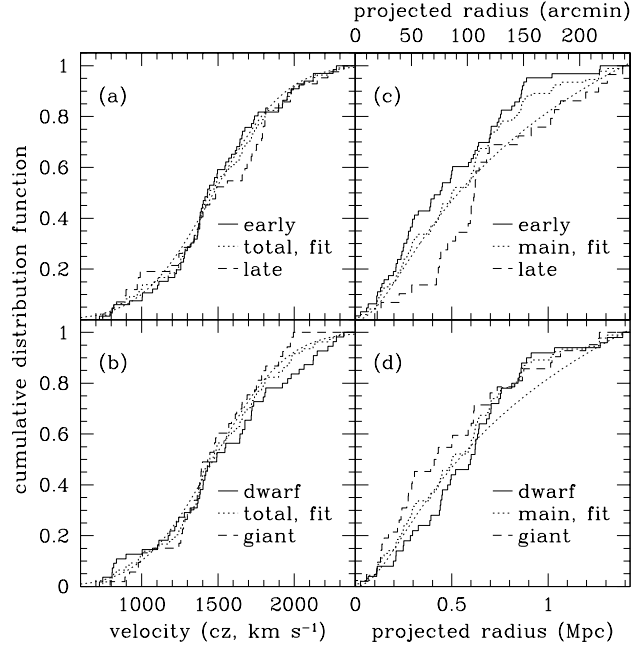


Fig. 1.— Cumulative distribution functions of Fornax galaxy velocities (a,b) for the total sample and projected radii (c,d) for the Fornax-main group only. In the top panels the total samples are compared to the early- and late-type subsamples and the bottom panels they are compared to the giant and dwarf subsamples. Also shown is the Gaussian fit to velocities of the total sample (a,b) and the King model fitted to the radial distribution of the whole cluster (Ferguson 1989) (c,d).

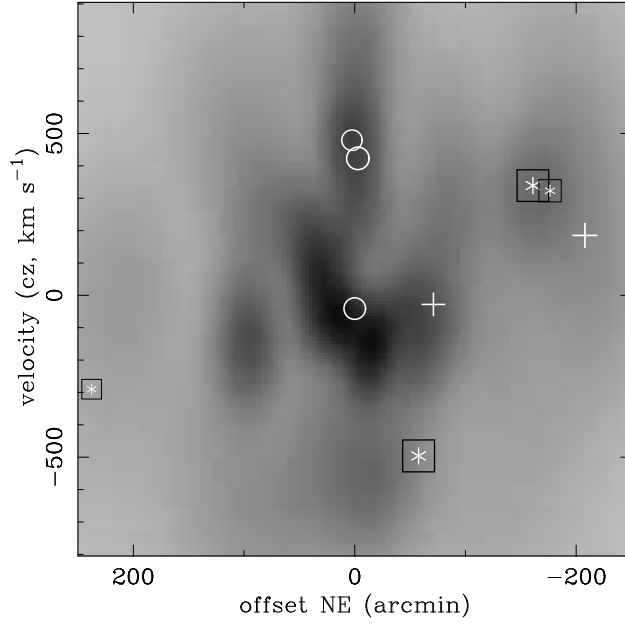


Fig. 2.— Adaptively-smoothed plot of the number density distribution of Fornax galaxies projected onto a plane of velocity against distance along a vector running South West to North East. The five brightest cluster galaxies are marked by circles for early-types (NGC 1380, NGC 1404 and NGC 1399 from top to bottom) and crosses for late-types (Fornax A and NGC 1365 from top to bottom). Also indicated by asterisks in squares are the four late-type galaxies with very strong star-formation activity (NGC 1341, FCC 35, FCCB 2144 and FCC 322, top to bottom).

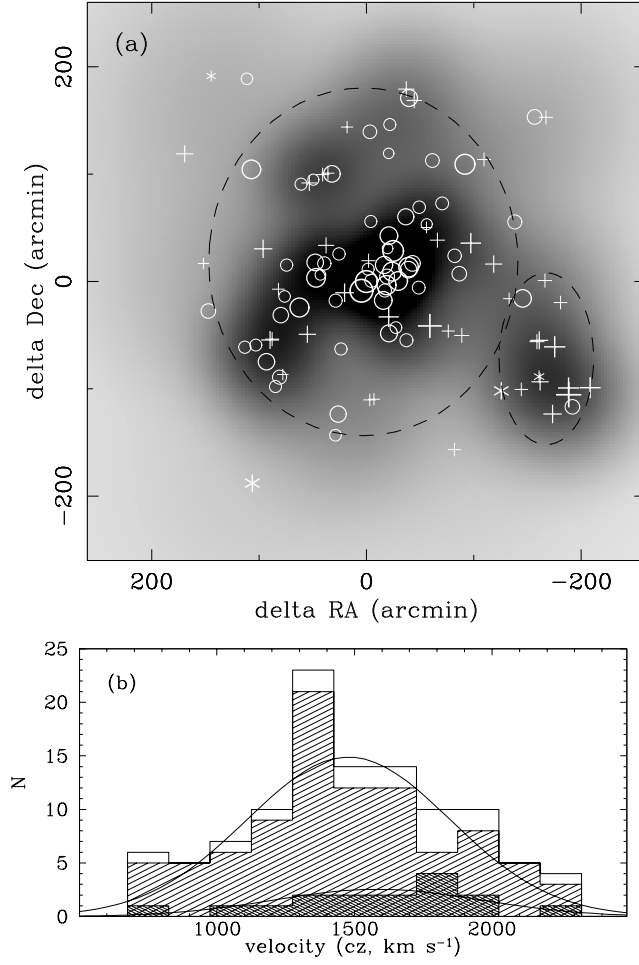


Fig. 3.— Partition of the Fornax system into two subclusters by the KMM algorithm. (a) Adaptively-smoothed plot of the number density distribution of Fornax galaxies on the sky (grey scale). The positions of cluster members are shown by circles (early-type galaxies) and crosses/asterisks (late-type galaxies). The asterisks indicate galaxies with high star formation rates. The symbol sizes are proportional to luminosity. The dashed ellipses are the 2σ limits of the subclusters. (b) Velocity histograms of the total sample (unshaded), the Fornax-main cluster (light shading) and the Fornax-SW subcluster (heavy shading) with the fitted Gaussians overlaid.

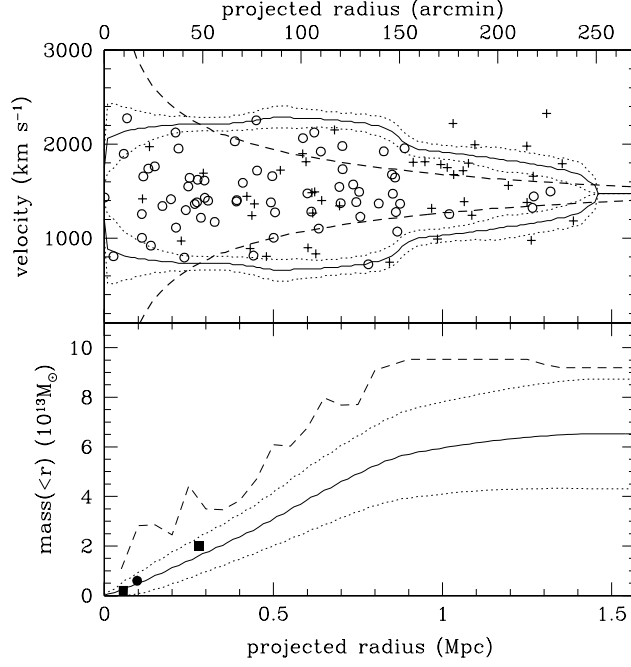


Fig. 4.— Top: radial velocities of Fornax galaxies plotted against projected radius from the cluster center. Early type galaxies are circles and late-types are crosses. The solid and dotted lines indicate the locus of the velocity amplitude $\mathcal{A}(x)$ and its uncertainties discussed in the text. The dashed lines indicate the locus of a caustic curve for a model with $\Omega_0 = 0.3$, $\sigma_v = 374 \text{ km s}^{-1}$, $r_{turn} = 2.4 \text{ Mpc}$. Bottom: Integrated mass profile of the Fornax Cluster derived by integrating the velocity amplitude profiles (solid and dotted lines), from the projected mass virial estimator (dashed line) and from X-ray observations by Ikebe et al. (1996) (squares) and Jones et al. (1997) (circle).